

A noise based novel strategy for faster SNN training

Chunming Jiang, Yilei Zhang
University of Canterbury, New Zealand

Abstract

Spiking neural networks (SNNs) are receiving increasing attention due to their low power consumption and strong bio-plausibility. Optimization of SNNs is a challenging task. Two main methods, artificial neural network (ANN)-to-SNN conversion and spike-based backpropagation (BP), both have their advantages and limitations. For ANN-to-SNN conversion, it requires a long inference time to approximate the accuracy of ANN, thus diminishing the benefits of SNN. With spike-based BP, training high-precision SNNs typically consumes dozens of times more computational resources and time than their ANN counterparts. In this paper, we propose a novel SNN training approach that combines the benefits of the two methods. We first train a single-step SNN by approximating the neural potential distribution with random noise, then convert the single-step SNN to a multi-step SNN losslessly. The introduction of Gaussian distributed noise leads to a significant gain in accuracy after conversion. The results show that our method considerably reduces the training and inference times of SNNs while maintaining their high accuracy. Compared to the previous two methods, ours can reduce training time by 65%-75% and achieves more than 100 times faster inference speed. We also argue that the neuron model augmented with noise makes it more bio-plausible.

1. Introduction

Spiking neural networks (SNNs) recently attracted increasing attention due to their biological plausibility. The SNN incorporates the concept of time into the model, and neurons in the SNN receive input spike trains that either increase or decrease their membrane potential. Through temporal accumulation, membrane potential may reach a specific firing threshold and neurons transmit information by firing discrete spike trains to neurons in the next layer. These characteristics emulate the information transmission and processing in the brain. It is therefore regarded as the next-generation neural network (Tavanaei et al., 2019).

Since SNNs use non-differentiable spikes as information carrying agents, gradient-based backpropagation (BP) that uses gradients to optimize synaptic connections and neuron parameters in ANNs is not directly applicable in SNNs. Thus, one of the main challenges is to train and optimize the network parameters in SNNs. At present, the available methods for training SNNs can be divided into three

categories: (1) unsupervised learning, (2) indirect supervised learning, (3) direct supervised learning.

In the first approach, weights are modulated to mimic synaptic interactions between biological neurons. A classic example is the spike time-dependent plasticity (STDP) (Diehl & Cook, 2015; Kheradpisheh et al., 2016; Querlioz et al., 2013). However, due to the reliance on local neuronal activity rather than global supervision, STDP-based unsupervised algorithms have been limited to training shallow SNNs and can only produce low accuracy on complex datasets (Han et al., 2020; Masquelier & Thorpe, 2007; Srinivasan et al., 2018).

In the second approach, an ANN model is first trained and then converted to a SNN with the same network structure, where the firing rate of the SNN neuron is approximated as the analog output of the ANN neuron. The ANN-to-SNN conversion has produced state-of-the-art (SOTA) performance in image recognition tasks (Roy et al., 2019).

The last approach is direct supervised learning, which uses a similar gradient descent technique used in ANNs to train SNNs directly. SpikeProp (Bohte et al., 2002) was the first BP-based supervised learning method for SNNs that uses a linear approximation to overcome the SNNs' non-differentiable threshold-triggered firing mechanism. Further works include Tempotron (Gutig & Sompolinsky, 2006), ReSuMe (Ponulak & Kasiński, 2010), and SPAN (Mohammed et al., 2012). However, they could only be used for training single-layer SNNs. A surrogate gradient algorithm proposed by (Wu et al., 2018) introduces a differentiable surrogate function to approximate the derivative of spiking activity. It executes spatio-temporal BP in the training phase and is widely applied to train deep SNNs.

Although the ANN-to-SNN conversion and surrogate gradient-based algorithm can train deep SNNs, there are some limitations. For the ANN-to-SNN conversion, training an ANN model is fast. Nevertheless, the approach requires considerable inference time (from hundreds to thousands of time steps) to approximate the analog outputs (Cao et al., 2015; Hunsberger & Eliasmith, 2015; Rueckauer et al., 2017; Sengupta et al., 2019; Stöckl & Maass, 2021), which leads to high memory consumption, larger latency and decreased energy efficiency, diminishing the benefits of SNNs (Deng & Gu, 2021; Roy et al., 2019; Severa et al.,

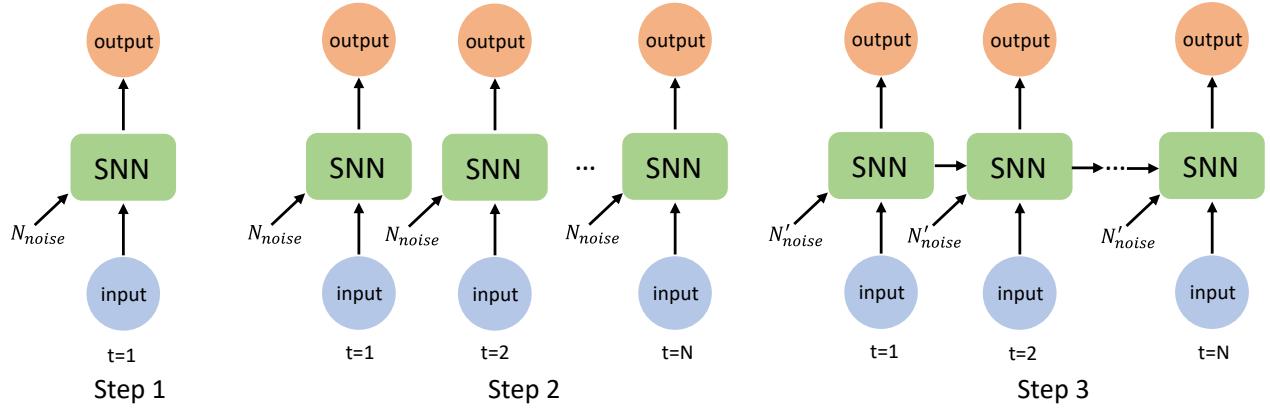


Fig.1 Three steps of our method to train a SNN model. Step 1, single-step SNN training with noise distribution N_{noise} . Step 2, copy N single-step SNNs and ensemble them together. N_{noise} varies over time-step t . Step 3, establish the temporal correlation among N different models.

2019). For the surrogate gradient-based algorithm, although it is possible to train SNNs with arbitrary time steps, the fewer the time steps, the lower the accuracy of the trained model would be. Training high accuracy SNNs with this approach often requires many times more training time and computational resources than training ANNs.

In this paper, we propose a novel SNN training method that combines the ANN-to-SNN conversion and direct training using the surrogate gradient. The method consists of two phrases: single-step SNN training and conversion to multi-step SNN. Specifically, during the training phase, a single-step SNN augmented with Gaussian noise is trained by surrogate gradient-based BP and then converted losslessly to a multi-step SNN model to promote its generalization capability. Our training technique greatly reduces not only training and inference time but also achieves a high accuracy, which significantly improves the efficiency of SNN.

The following summarizes the primary contributions of this paper:

- 1) We propose a novel SNN training algorithm by introducing a noise distribution, which speeds up the training and inference time of SNN.
- 2) We compare our method's training and inference time with those of current SNN training methods. The experiments demonstrate that our method is 3-5 times faster for training than the surrogate-gradient based method, and more than 100 times faster than the ANN-to-SNN conversion for inference.
- 3) We argue that introducing noise in SNN has biological plausibility.

2. Methods

2.1. Leaky Integrate-and-Fire model

The leaky Integrate-and-Fire (LIF) model is a fundamental unit in SNNs. It is a simplified representation of biological neurons that describes the non-linear relationship between input and output. The LIF neuron receives spikes over a specific period and it integrates them into its membrane potential, whose dynamics are governed by

$$H(t) = \lambda \cdot V(t-1) + \sum_i w_i \cdot S_i(t) \quad (1)$$

$$S(t) = \begin{cases} 1, & H(t) > V_{th} \\ 0, & H(t) \leq V_{th} \end{cases} \quad (2)$$

$$V(t) = H(t)(1 - S(t)) + V_{reset} \cdot S(t) \quad (3)$$

where $H(t)$ and $V(t)$ represent the membrane potentials before and after triggering a spike at time t , respectively. λ represents the decay factor with a value of 0.5. $S(t)$ denotes the output of a neuron at time t , which equals 1 if there is a spike and 0 otherwise. $w_i \cdot S_i(t)$ is the weighted input of i -th neuron in the last layer at time step t . When the membrane potential of the LIF neuron reaches the firing threshold V_{th} ($= 1$), the neuron fires one spike and the membrane potential is reset to the resting potential V_{reset} (here is 0).

2.2. Training single-step SNN and converting to multi-step SNN

We first train the single-step SNN with $T = 1$ and then convert it to a multi-step SNN with $T = N$. When the total simulation step $T = 1$, the time dimension disappears and the network propagates forward only once. Consequently, the single-step SNN is actually an ANN with a Heaviside

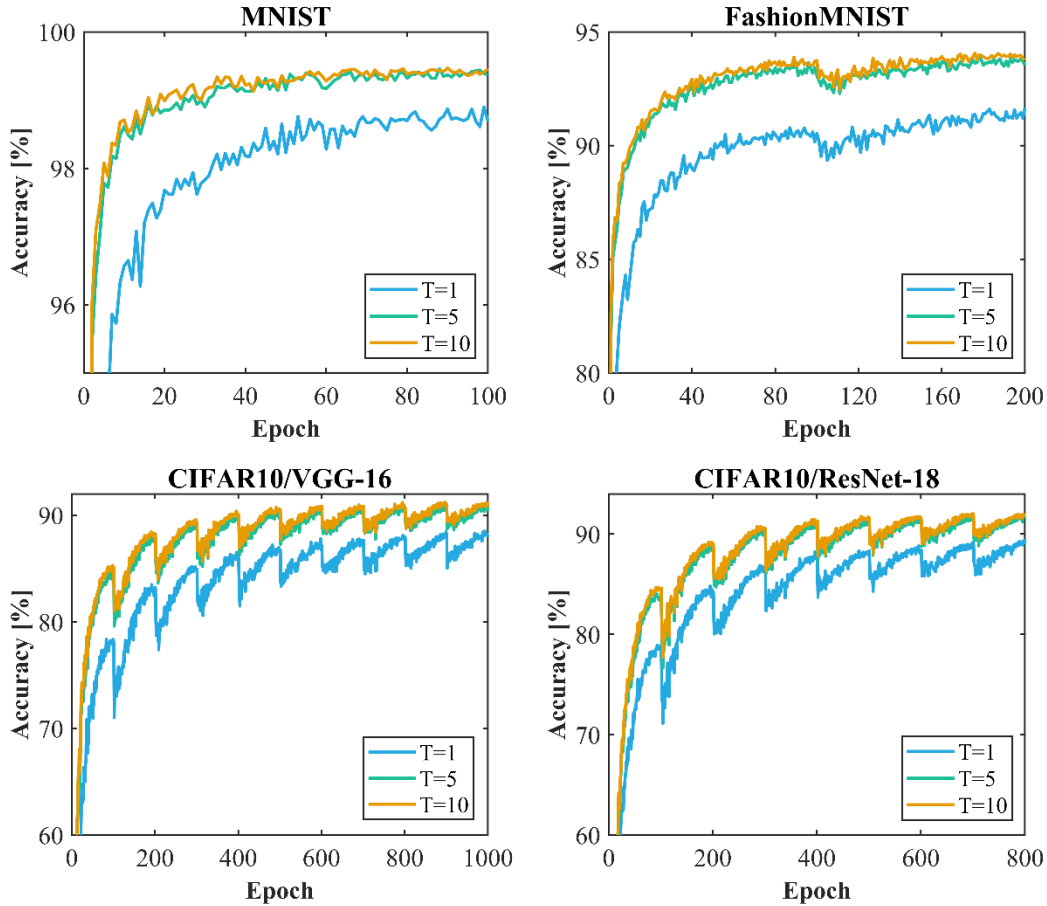


Fig.2 Inference accuracy of models on different datasets with $T = 1, 5, 10$ while training with N_{noise} .

Table 1 Network structures and training epoch for different datasets.

Dataset	Epoch	Network structure
MNIST	100	64C3-AP2-128C3-AP2-128C3-AP2-512FC-10FC
Fashion - MNIST	200	
CIFAR-10	1000	VGG-16
	800	ResNet-18

Note: nC3—Convolutional layer with n output channels, kernel size = 3 and stride = 1, AP2—2D average-pooling layer with kernel size = 2 and stride = 2. FC—Fully connected layer.

step function used as the activation function. Equation (1) is formulated as

$$H = \sum_i w_i \cdot S_i \quad (4)$$

Comparing Equations (1) and (2), the output of the multi-step SNN depends on both the input and the accumulated potential, while the output of a single-step SNN depends only on the input.

Due to the absence of the potential accumulation term in Equation (4) compared with Equation (1), we introduce a noise distribution N_{noise} representing the missing accumulated membrane potential during training the single-

step SNN in order to perform the conversion into a multi-step SNN later, as Equation (5) shows. In particular, we assume that N_{noise} is a Gaussian distribution and distributes in each layer of the network independently. Thus, the dynamic of the neuron in a single-step SNN could be described by

$$H = N_{noise} + \sum_i w_i \cdot S_i \quad (5)$$

Our method consists of three following steps:

Step 1: Train the single-step SNN with Gaussian noise (see step 1 in Figure 1).

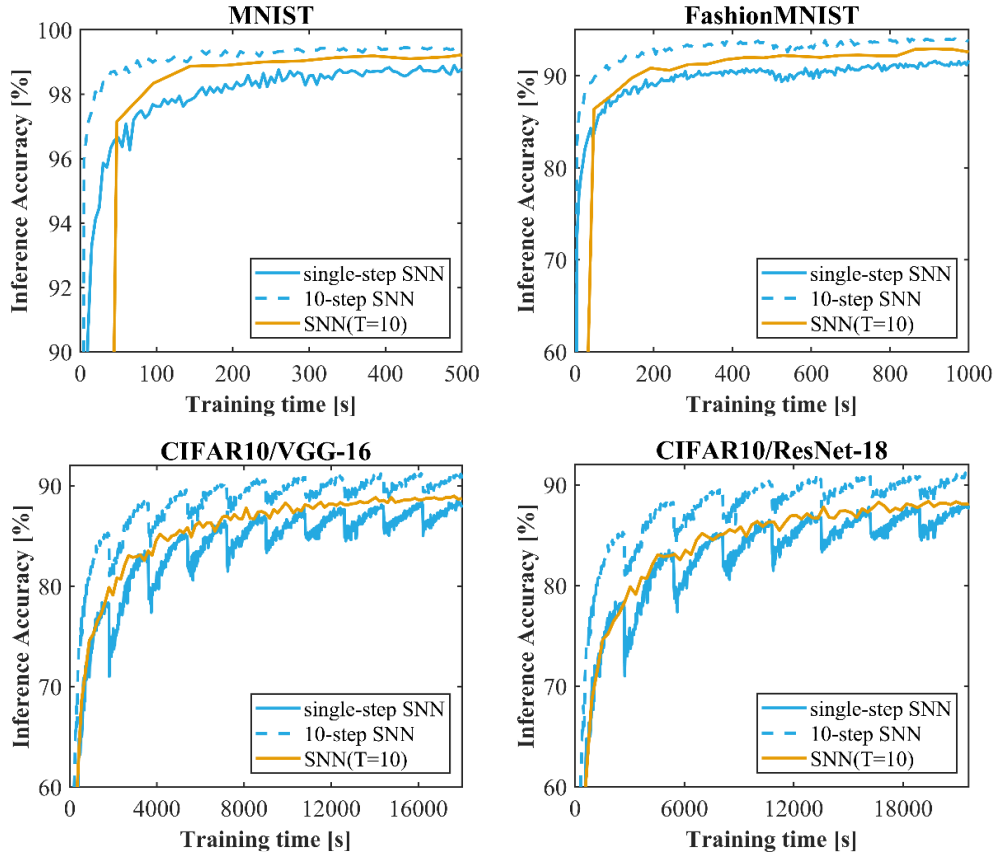


Fig.3 Training speed of SNNs when directly training an SNN($T=10$) by the surrogate gradient approach versus training a 10-step SNN by our approach.

Step 2: Extend the temporal dimension from $T = 1$ to $T = N$ by directly modifying the value of T . This action means that we copy N single-step SNN and ensemble them together (see step 2 in Figure 1). For each individual, the inputs are the same. The average output of all individuals is the output of the ensemble model.

Step 3: Add the potential accumulation term using Equation (6) to establish the temporal correlation (see step 3 in Figure 1). The dynamic of SNN model after step 2 is formally different from the real SNN's dynamic because it lacks the process of potential accumulation and the temporal correlation among different time step t . Consequently, we must add the item $\lambda \cdot V(t-1)$ to keep the formal consistency with Equation (1). We decompose N_{noise} into:

$$N_{noise} = N(\lambda \cdot V(t-1)) + N'_{noise} \quad (6)$$

N_{noise} could be represented as the addition of two Gaussian distribution items: the accumulated membrane potential distribution and the new noise distribution.

For the first item, we normalize $\lambda \cdot V(t-1)$ according to Equations (7)-(9) to approximate a Gaussian distribution $N(\lambda \cdot V(t-1))$.

$$A = \lambda \cdot V(t-1) \quad (7)$$

$$\hat{A} = \frac{A - \mu}{\sigma} \quad (8)$$

$$N(\lambda \cdot V(t-1)) = \frac{\hat{A}}{\alpha \cdot \max(\text{abs}(\hat{A}))} + \beta \quad (9)$$

Equation (8) converts the membrane potential distribution to a standard normal distribution approximately. μ and σ are the mean and standard deviation of A , respectively. Equation (9) guarantees that the potential distribution in each layer have the mean β and distributes between the interval $(-1/\alpha, 1/\alpha)$. By changing the values of α and β , we are able to change the mean and range of the distribution. ($\max()$ and $\text{abs}()$ represent taking the maximum value and absolute value, respectively.)

For the second item N'_{noise} , we simply set it as a random Gaussian distribution. The mean and range of N'_{noise} also depends on α and β , because we need to guarantee that the addition of two items in Equation (6) almost have the same mean and range as N_{noise} to avoid conversion loss.

The reason why we must introduce and keep the random noise distribution is that introducing the noise is equivalent to ensemble an infinite number of random models and helps promote accuracy during conversion to multi-step SNN.

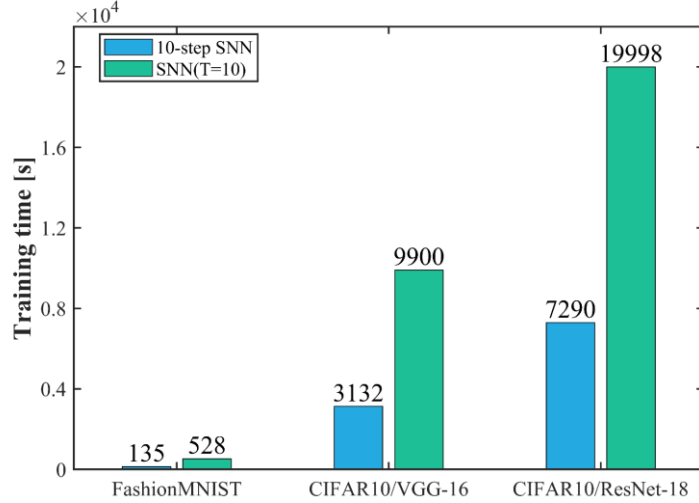


Fig.4 Training time of SNNs when directly training an SNN($T=10$) by the surrogate gradient approach versus training a 10-step SNN by our approach. The benchmark inference accuracy of the three models is 92%, 88%, and 90%, respectively.

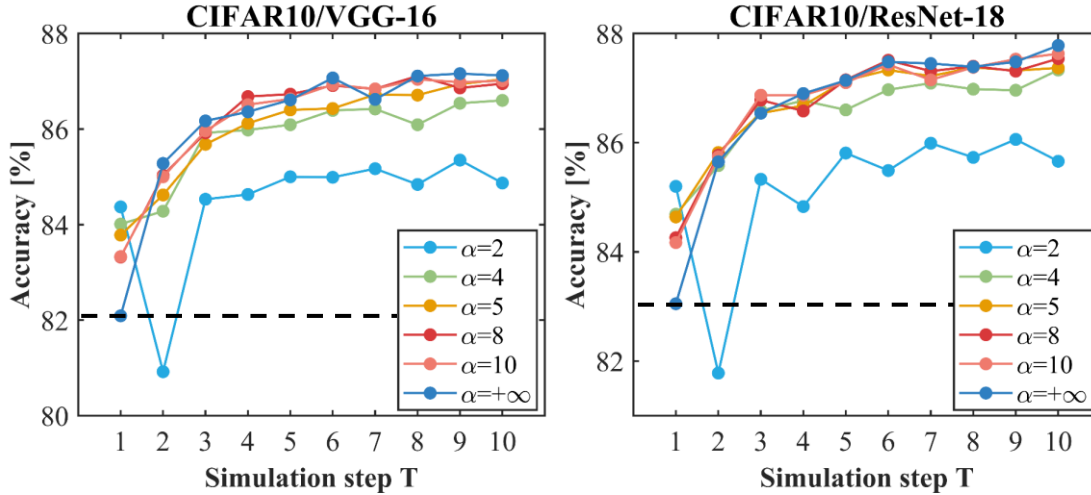


Fig.5 The impact of α on CIFAR10/VGG-16 and CIFAR10/ResNet-18. The black dotted line represents the accuracy of trained single-step SNN.

Because we introduce a random distribution when training single-step SNNs, the model generalizes well under different “assumed previous membrane potentials”. As we increase the time step, the SNN with T simulation steps can be seen as a model consisting of T sets of models.

It is well known that a SNN model with more simulation steps T can increase performance. However, training a SNN with large T directly would increase not only the training and inference time but also the memory by T folds, so it is not very practical. The approach that we suggest can instantly construct a SNN model with large T with much less memory cost. The idea of introducing noise to generate an ensemble model was proposed in (Liu et al., 2018) and used for adversarial defense of ANN models. To the best of

our knowledge, we are the first to use it in training and inference acceleration of SNNs.

3. Results and discussions

We conduct our experiments as Table 1 shows. SNNs are trained with MSE loss and Adam (Kingma & Ba, 2014) optimizer. The initial learning rate is set to $1e-4$. The cosine annealing warm restart (Loshchilov & Hutter, 2016) learning rate schedule with $T_{max} = 100$ adjusts the learning rate over training. Unless specified, all results are generated by default for $\alpha = 4$, $\beta = 0.5$, and N_{noise} in the range $[0, 1]$.

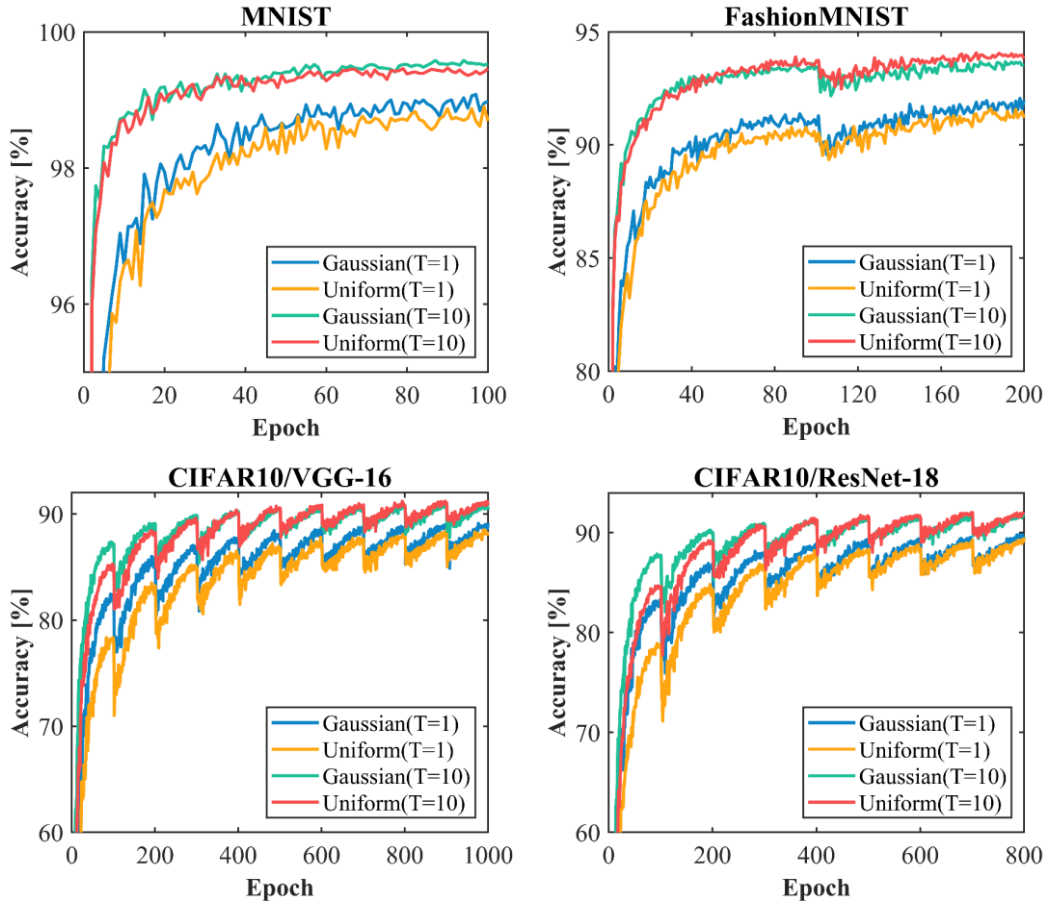


Fig.6 Inference accuracy of models on different datasets with $T = 1, 10$ while training using Gaussian noise and uniform noise, respectively.

3.1. Inference accuracy

In Figure 2, we plot the inference accuracy of single-step SNNs on different datasets and the inference accuracy of multi-step SNNs with total simulation step $T = 5$ and $T = 10$, respectively. It can be shown that as T increases, the accuracy of the SNN improves dramatically. The simulation step T could be directly converted to any values in real time.

3.2. Comparison of training and inference time with related work

In Figure 3, we compare the training speed of SNNs when training an SNN($T=10$) with a surrogate gradient versus training a single-step SNN and then extending to a 10-step SNN. Clearly, our method is substantially faster than directly training an SNN($T=10$) using the surrogate gradient, and in the same amount of time, it achieves higher accuracy. To intuitively assess the difference in training time, we selected a benchmark inference accuracy for each model and halted training when the benchmark inference accuracy was

achieved. The benchmark inference accuracy of the three models is 92%, 88%, and 90%, respectively. As shown in Figure 4, on FashionMNIST our method takes only 135s to reach the benchmark accuracy when SNN($T=10$) takes 528s, which saves about 75% of the time. In CIFAR10/VGG-16, our method requires 3132s, whereas SNN($T=10$) requires 9900s, a time savings of about 70%. In CIFAR10/ResNet-18, our model requires 7290s while SNN($T=10$) requires 19998s, a time savings of approximately 65%. Also, with single-step SNN, we can choose a larger batch size and thus achieve faster parallel training. It is more convenient and feasible for groups that lack sufficient computational resources.

For inference time, we compare current advanced methods listed in Table 2 with our method. As demonstrated, the accuracy of extending to multi-step SNN (no more than 10 time steps) is able to attain an approximate accuracy of ANN-to-SNN conversion methods. In contrast, ANN-to-SNN conversion requires hundreds to thousands of time steps, which is hundreds of times slower than our method.

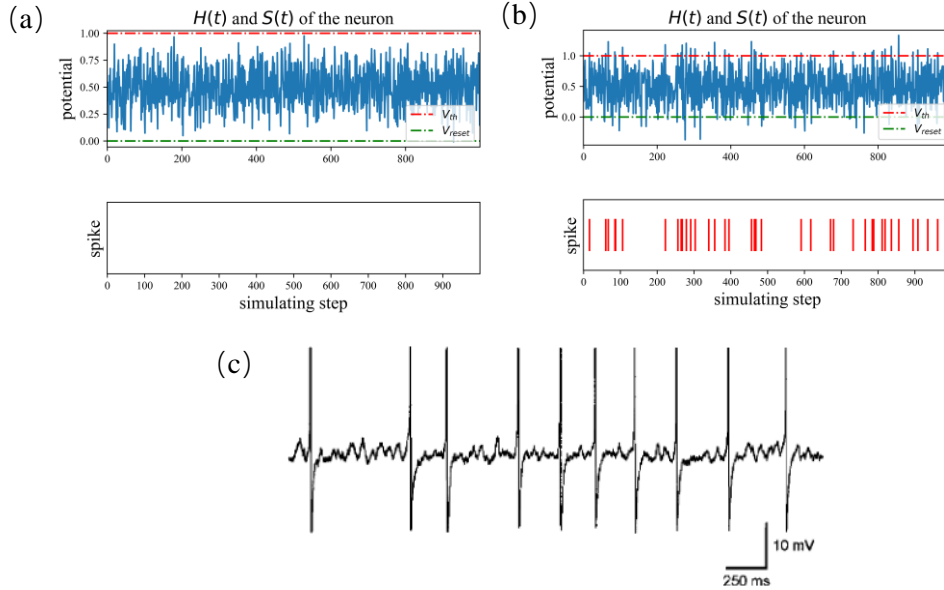


Fig.7 (a) Neural potential dynamic in the absence of input. (b) Neural potential dynamic when receiving input. (c) Subthreshold membrane potential oscillation. Source: Figure (c) is cited from (Boehmer et al., 2000).

Table 2 Inference time comparison between our work and related work

Author	Method	Inference time	MNIST	FashionMNIST	CIFAR10
(Wu et al., 2019)	Spike-based BP	12	-	-	90.53%
(Rathi & Roy, 2021)	Spike-based BP	10	-	-	93.44%
(Cheng et al.)	Spike-based BP	20	99.50%	92.07%	93.5%
(Severa et al., 2019)	Spike-based BP	1	99.53%	-	84.67%
(Sengupta et al., 2019)	ANN-SNN	2500	-	-	91.46%
(Han et al., 2020)	ANN-SNN	2048	-	-	91.36%
(Diehl et al., 2015)	ANN-SNN	2500	-	-	91.89%
(Lee et al., 2020)	ANN-SNN	50/100	99.59%	-	90.95%
(Stöckl & Maass, 2021)	Hybrid	500	-	-	92.42%
(Rathi et al., 2020)	Hybrid	200	-	-	92.02%
Ours	Hybrid	5	99.61%	93.89%	91.82%
Ours	Hybrid	10	99.64%	94.07%	92.07%

Compared with spike-based BP methods, our method also requires fewer time steps to reach high accuracy.

3.3. The impact of α

With Equations (6) and (9), we know that the parameter α controls the range of noise fluctuation N'_{noise} . Here, we attempt to alter the value of α to observe how the model's performance varies.

We plot the conversion accuracy for different values of α in Figure 5. When α is equal to 2, the potential range is $[0, 1]$, so the noise term N'_{noise} does not exist any more. It can be seen that there is a very slight improvement in accuracy with increasing time steps. In contrary, when N'_{noise} is present, the accuracy improvement is obvious and the different α values make models converge to close

accuracy. These results indicate that noise plays the vital role in enhancing the accuracy of conversion.

When α is positive infinity, the range of noise N'_{noise} is $[0, 1]$, membrane potential item disappears and the result equals to the outcome of step 2. The conversion from step 2 to step 3 has minor accuracy gap according to the figures.

3.4. The impact of noise type

In the previous sections, all of our experiments were performed by training the SNN model with Gaussian noise. In order to investigate whether it is only the uniform noise that brings the improvement of model accuracy, we replace the Gaussian noise with uniform noise during training to observe the effect of the noise type on models. As shown in Figure 6, we trained CIFAR-10 with uniform noise on both

VGG-16 and ResNet-18 models. Models trained by uniform noise behave the same as with uniform noise, i.e., the accuracy is significantly improved when models are extended to multi-step SNNs. For single-step SNNs, models with Gaussian noise reach the higher accuracy than those with uniform noise. But after conversion, the gap is not obvious any more.

3.5. Biological plausibility of uniform noise distribution in neuron

It is believed to be more biologically plausible when we keep some part of noise during conversion, as there exists lots of kinds of noise in biological neural system. We plot the dynamic of the spiking neuron in Figures 7(a) and (b). Figure 7(a) depicts the neural potential dynamic in the absence of input. The potential oscillates between the reset potential and the threshold, but no spikes fire. In Figure 7(b), when a neuron receives inputs, it begins to accumulate potential and fires spike. Such behavior is thought to be similar to the form of subthreshold neural oscillation mechanism in biological neurons. Neural oscillations are rhythmic patterns of activity generated by the neurological system (Başar, 2013). Many cognitive activities, including information transfer, perception, and memory, are believed to be related with neural oscillations. These oscillations are mostly caused by the interaction between individual neurons. Neural oscillation can emerge as oscillating membrane potentials or rhythmic action potentials in individual neurons. Subthreshold membrane potential oscillations are membrane oscillations that are below the firing threshold and hence cannot directly initiate action potentials. However, they can aid in sensory signal processing. As a result of subthreshold membrane potential oscillations, sensory systems, particularly for vision and smell, evolve. Subthreshold membrane potential oscillation (see Figure 7(c)) in the visual system helps process visual input and adjust to sensory input (Purves et al., 2008). Additionally, oscillatory activity influences excitatory postsynaptic potentials, refining post-neural activities (Desmaisons et al., 1999).

4. Conclusion

In this paper, we propose a novel way of training SNNs that achieves accuracy improvement in multi-step SNNs by fitting the neural network to noise, which greatly spares the training and inference time of SNNs and allows fast training of SNNs with arbitrary simulation time compared to previous methods. Our approach combines the advantages of both direct training of SNN and ANN-to-SNN conversion. With a good balance of accuracy and training time, and a great saving of computational resources, this method can be used to train large SNNs quickly or SNN pre-

training. The inclusion of noise is also proved to be more consistent with the dynamic mechanism of biological neurons. These points make our method promising for training deep SNNs in the future.

References

- Başar, E. (2013). Brain oscillations in neuropsychiatric disease. *Dialogues in clinical neuroscience*, 15(3), 291.
- Boehmer, G., Greffrath, W., Martin, E., & Hermann, S. (2000). Subthreshold oscillation of the membrane potential in magnocellular neurones of the rat supraoptic nucleus. *The Journal of physiology*, 526(Pt 1), 115.
- Bohte, S. M., Kok, J. N., & La Poutre, H. (2002). Error-backpropagation in temporally encoded networks of spiking neurons. *Neurocomputing*, 48(1-4), 17-37.
- Cao, Y., Chen, Y., & Khosla, D. (2015). Spiking deep convolutional neural networks for energy-efficient object recognition. *International Journal of Computer Vision*, 113(1), 54-66.
- Cheng, X., Hao, Y., Xu, J., & Xu, B. LISNN: Improving Spiking Neural Networks with Lateral Interactions for Robust Object Recognition. IJCAI,
- Deng, S., & Gu, S. (2021). Optimal Conversion of Conventional Artificial Neural Networks to Spiking Neural Networks. *arXiv preprint arXiv:2103.00476*.
- Desmaisons, D., Vincent, J.-D., & Lledo, P.-M. (1999). Control of action potential timing by intrinsic subthreshold oscillations in olfactory bulb output neurons. *Journal of Neuroscience*, 19(24), 10727-10737.
- Diehl, P. U., & Cook, M. (2015). Unsupervised learning of digit recognition using spike-timing-dependent plasticity. *Front Comput Neurosci*, 9, 99. <https://doi.org/10.3389/fncom.2015.00099>
- Diehl, P. U., Neil, D., Binas, J., Cook, M., Liu, S.-C., & Pfeiffer, M. (2015). Fast-classifying, high-accuracy spiking deep networks through weight and threshold balancing. 2015 International Joint Conference on Neural Networks (IJCNN),
- Gutig, R., & Sompolinsky, H. (2006, Mar). The tempotron: a neuron that learns spike timing-based decisions.

- Han, B., Srinivasan, G., & Roy, K. (2020). RMP-SNN: Residual Membrane Potential Neuron for Enabling Deeper High-Accuracy and Low-Latency Spiking Neural Network. Proceedings of the IEEE/CVF Conference on Computer Vision and Pattern Recognition,
- Hunsberger, E., & Eliasmith, C. (2015). Spiking deep networks with LIF neurons. *arXiv preprint arXiv:1510.08829*.
- Kheradpisheh, S. R., Ganjtabesh, M., & Masquelier, T. (2016). Bio-inspired unsupervised learning of visual features leads to robust invariant object recognition. *Neurocomputing*, 205, 382-392.
- Kingma, D. P., & Ba, J. (2014). Adam: A method for stochastic optimization. *arXiv preprint arXiv:1412.6980*.
- Lee, C., Sarwar, S. S., Panda, P., Srinivasan, G., & Roy, K. (2020). Enabling spike-based backpropagation for training deep neural network architectures. *Frontiers in neuroscience*, 14.
- Liu, X., Cheng, M., Zhang, H., & Hsieh, C.-J. (2018). Towards robust neural networks via random self-ensemble. Proceedings of the European Conference on Computer Vision (ECCV),
- Loshchilov, I., & Hutter, F. (2016). Sgdr: Stochastic gradient descent with warm restarts. *arXiv preprint arXiv:1608.03983*.
- Masquelier, T., & Thorpe, S. J. (2007). Unsupervised learning of visual features through spike timing dependent plasticity. *PLoS Comput Biol*, 3(2), e31.
- Mohammed, A., Schliebs, S., Matsuda, S., & Kasabov, N. (2012). Span: Spike pattern association neuron for learning spatio-temporal spike patterns. *International journal of neural systems*, 22(04), 1250012.
- Ponulak, F., & Kasiński, A. (2010). Supervised learning in spiking neural networks with ReSuMe: sequence learning, classification, and spike shifting. *Neural computation*, 22(2), 467-510.
- Purves, D., Cabeza, R., Huettel, S. A., LaBar, K. S., Platt, M. L., Woldorff, M. G., & Brannon, E. M. (2008). *Cognitive neuroscience*. Sunderland: Sinauer Associates, Inc.
- Querlioz, D., Bichler, O., Dollfus, P., & Gamrat, C. (2013). Immunity to device variations in a spiking neural network with memristive nanodevices. *IEEE Transactions on Nanotechnology*, 12(3), 288-295.
- Rathi, N., & Roy, K. (2021). Diet-snn: A low-latency spiking neural network with direct input encoding and leakage and threshold optimization. *IEEE transactions on neural networks and learning systems*.
- Rathi, N., Srinivasan, G., Panda, P., & Roy, K. (2020). Enabling deep spiking neural networks with hybrid conversion and spike timing dependent backpropagation. *arXiv preprint arXiv:2005.01807*.
- Roy, K., Jaiswal, A., & Panda, P. (2019). Towards spike-based machine intelligence with neuromorphic computing. *Nature*, 575(7784), 607-617.
- Rueckauer, B., Lungu, I.-A., Hu, Y., Pfeiffer, M., & Liu, S.-C. (2017). Conversion of continuous-valued deep networks to efficient event-driven networks for image classification. *Frontiers in neuroscience*, 11, 682.
- Sengupta, A., Ye, Y., Wang, R., Liu, C., & Roy, K. (2019). Going deeper in spiking neural networks: Vgg and residual architectures. *Frontiers in neuroscience*, 13, 95.
- Severa, W., Vineyard, C. M., Dellana, R., Verzi, S. J., & Aimone, J. B. (2019). Training deep neural networks for binary communication with the whetstone method. *Nature Machine Intelligence*, 1(2), 86-94.
- Srinivasan, G., Panda, P., & Roy, K. (2018). Stdp-based unsupervised feature learning using convolution-over-time in spiking neural networks for energy-efficient neuromorphic computing. *ACM Journal on Emerging Technologies in Computing Systems (JETC)*, 14(4), 1-12.
- Stöckl, C., & Maass, W. (2021). Optimized spiking neurons can classify images with high accuracy through temporal coding with two spikes. *Nature Machine Intelligence*, 3(3), 230-238.
<https://doi.org/10.1038/s42256-021-00311-4>
- Tavanaei, A., Ghodrati, M., Kheradpisheh, S. R., Masquelier, T., & Maida, A. (2019). Deep learning in spiking neural networks. *Neural Networks*, 111, 47-63.

- Wu, Y., Deng, L., Li, G., Zhu, J., & Shi, L. (2018). Spatio-Temporal Backpropagation for Training High-Performance Spiking Neural Networks. *Front Neurosci*, *12*, 331. <https://doi.org/10.3389/fnins.2018.00331>
- Wu, Y., Deng, L., Li, G., Zhu, J., Xie, Y., & Shi, L. (2019). *Direct training for spiking neural networks: Faster, larger, better* Proceedings of the AAAI Conference on Artificial Intelligence,